# JOURNAL OF ENGINEERING RESEARCH

Refereed and issued twice annually by the
Faculty of Engineering - University of Tripoli



Issue 30 September 2020

# MODELING OF AIDING MIXED CONVECTION IN PARTIALLY HEATED VERTICAL CHANNLES

**Musa M. Radwan and Akram A. Alhrari***

Department of Petroleum Engineering, University of Tripoli, Tripoli, Libya
*Department of Mechanical Engineering, Zawia University, Zawia, Libya
Email: M.Radwan@uot.edu.ly

**الملخص**

تم في هذه الورقة دراسة الحمل الحراري المختلط للانسياب الرقائقي في قناة رأسية مسخنة جزئياً بتطبيق فيض حراري منتظم محيطياً على الجزء الأسفل من القناة $L_h/D_h = 10$ وعزل الجزء المتبقي من القناة $L_i/D_h = 90$ وذلك باستخدام طريقة (Finite-control volume method) لاستنباط توزيع درجات الحرارة والسرعات للمائع المتدفق انسيابياً عند مقاطع مختلفة من محور القناة متضمناً الجزء المعزول حرارياً. وكذلك شكل خطوط التدفق الانسيابية (streamlines) عند قيم مختلفة لـGrashof number. تم حل معادلات الاستمرارية (continuity) وقوة الدفع (momentum) والطاقة آنيا باستخدام الطريقة العددية المشار إليها حيث تم دراسة تأثير طول الجزء المسخن على نمط التدفق وأداء نقل الحرارة عند قيمة ثابتة لـ Grashof number وقد أخذ في الاعتبار تأثير الانتشار المحوري (axial diffusion) في معادلات الزخم والطاقة وتم إعطاء اهتمام خاص إلى النسبة $Gr/Re^2$ وتأثيرها على المجالين الهيدروديناميكي والحراري خصوصا في منطقة مدخل القناة عند قيم مختلفة لـ Grashof number وقيمة محددة لعدد رينولد Re = 500, $10^5 \le Gr \le 10^7$. حيث يحدث انعكاس التدفق بالقرب من المحور في حالة التدفق المتصاعد الساخن. في هذه الورقة تم تعيين وعرض خطوط الانسياب في القناة والانسياب الايزوتيرمي (isotherms) وكذلك حساب توزيع درجات الحرارة والسرعة وعدد نسلت (Nusselt) الموضعي ومعامل الاحتكاك.

**ABSTRACT**

In this paper laminar mixed convection in partially heated vertical channel was investigated numerically. The temperature profiles at various axial locations, axial velocity profile in the heated part of the channel and streamlines for aiding buoyancy flow are presented. The case of aiding mixed convection is considered, with the lower part of the channel is subjected to uniform heat flux. Conservation equations of continuity, momentum and energy were solved simultaneously using Finite volume method. The effect of the length of the heated section on the flow pattern and heat transfer performance is investigated for given Grashof numbers. The influence of axial diffusion and it's relevant to flow reversal at the entrance region of the channel was taken into account in the momentum and energy equations and particular attention is given to the ratio $Gr / \mathrm{Re}^2$.

The effect of aiding bouncy forces on the hydrodynamic and thermal fields was examined for air with Re = 500, $10^5 \le Gr \le 10^7$. Reversal Flow was observed near the axis for aiding buoyancy flow. Streamlines in the channel, isotherms, temperature distribution, and velocity profiles, local Nusselt number and friction factor were presented. The numerical results presented revealed some interesting features which may be summarized as: (i) the effects of the heated part of the channel on the hydrodynamic and thermal fields are demonstrated for $\left| \mathrm{Gr} \right| \ge 10^5$ for aiding flow. (ii) Nusselt number approaches the asymptotic value at the vicinity of the channel wall for $\mathrm{Gr} \le 10^5$. For Gr

$\geq 10^6$ the Boussinesq approximation over predicts the overall heat transfer rate. (iii) For Gr up to $4x10^5$ The Boussinesq approximation still predicts reasonably the heat transfer rate. In general, the heated section modifies the flow field and hence the wall convective heat transfer.

**KEYWORDS:** Mixed convection; Flow in Channel; Heat fluxes; Finite volume

## INTRODUCTION

The importance of mixed convection in ducts originates from its wide range of practical applications, including cooling of discrete heat sources mounted on electronic equipment's, as well as the design of compact heat exchangers, solar collectors and cooling of voltaic cells. Numerous theoretical and experimental investigations concerning fluid flow in ducts of various shapes are available in the literature, Aung [1], Gebhart et al [2], Incropera [3] and Beijan [4]. Convection heat transfer may be classified according to the type of flow; heat is transferred by forced convection when external means such pumps or fans are used to pump a fluid over a solid surface. In contrast, natural or free convection occurs when the flow is induced by bouncy forces, due to density gradient as a result of temperature variation in the fluid. In addition, mixed convection, natural and forced may exist simultaneously if velocities associated with the forced flow are small and bouncy forces are large hence a secondary flow that is comparable to the imposed forced flow could be induced. Under this conditions the axial velocity may increase near the channel walls and decrease within the core region with possible existence of flow recirculation in the entry region for large bouncy forces [5, 6]. The effect of bouncy on heat transfer in a forced flow is strongly influenced by the direction of the bouncy force relative to that of the flow. These are (i) aiding (assisting flow), (ii) opposing flow, (iii) transverse flow, it is well known that heat transfer is enhanced by aiding and opposing flow but it is reduced for the transverse case. This work, considers the effect of thermal bouncy on the flow field commonly termed as bouncy aiding or assisting mixed convection. Recently, considerable research including numerical and analytical studies has been conducted [7- 9], in particular for flows in horizontal and vertical tubes. In these studies, the Boussinesq approximation has been suggested and implemented, which is based on two aspects, first the physical properties of the fluid are assumed constant except for the density. Second, the density variation in the continuity equation is ignored, but it is expressed as a linear function of temperature in the bouncy terms [10].

In the last decades with the availability of high speed computing facilities, it has been possible to analyze the validity of the constant property assumption in modeling convection heat transfer problems [11]. The validity of Boussienq approximation has been investigated by Giorgini and Gray [12] where the case of natural convection for gases and liquids between two parallel isothermal surfaces has been investigated and the results of their study has revealed the validity of the Boussienq approximation for small temperature gradients. However, for large temperature difference, the numerical solution become unstable and deviates from experimental data. Despite the fact that many works dealing with internal natural convection flow [13-16], relatively little work has been conducted to investigate the flow of air in partially heated vertical channel with mixed convection. Few works found in the literature are those of Aung [17], who has solved numerically the momentum and energy equations for upward heated flow of an ideal gas inside a vertical concentric annulus. However, the validity of Boussienq approximation was not included in their model. Nesserdine [18] has investigated the variable property

flow model of partially heated tube and compare the results with Boussienq approximation model; the results of the two models were very close for low to moderate Grashof number. In the present work, we have presented a model for aiding mixed convection flow of air in partially heated vertical channel. Numerical results for flow and thermal fields are presented and the effect of the applied heat flux is investigated.

## MATHEMATICAL FORMULATION

This work is concerned with developing mixed convection flow in the entrance region of a vertical channel; the physical model under consideration is illustrated in Figure (1). The channel wall is heated with uniform heat flux over a finite length $L_h/D_h$ and insulated elsewhere. The fluid enters the channel with uniform velocity and temperature. Simulations were performed for air as the working fluid and corresponding to the following $\mathrm{Re} = 500$ , $\mathrm{Pr} = 0.7$ , $10^5 \le |Gr| \le 10^7$, and $L_h / D_h = 10$. Note that the insulated section of the channel is considered long enough ($L_i / D_h = 90$) to allow for fully devolved profiles , even for high $Gr$.

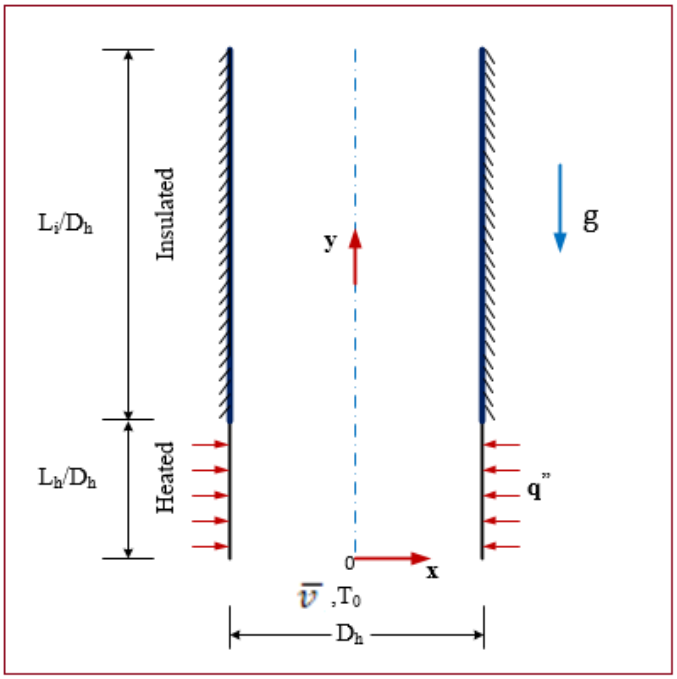


**Figure 1: Schematic representation of the phsiycal model.**

The mathematical model of the problem is constructed taking into account the following simplifying assumptions:

- The flow is steady, laminar and two dimensional
- The flow is Incompressible and Newtonian.
- The viscous dissipation and compression work are neglected

Based on the above mentioned assumptions, the governing equations of the flow were derived from the basic conservation principles of mass, momentum, and energy and can be written as [3,4]:

$$\frac{\partial(\rho u)}{\partial x} + \frac{\partial(\rho v)}{\partial y} = 0 \qquad (1)$$

$$\frac{\partial(\rho uu)}{\partial x}+\frac{\partial(\rho uv)}{\partial y}=-\frac{\partial p}{\partial x}+\mu\left[\frac{\partial^2 u}{\partial x^2}+\frac{\partial^2 u}{\partial y^2}\right] \quad (2)$$

$$\frac{\partial(\rho uv)}{\partial x}+\frac{\partial(\rho vv)}{\partial y}=-\frac{\partial p}{\partial y}+\mu\left[\frac{\partial^2 v}{\partial x^2}+\frac{\partial^2 v}{\partial y^2}\right]+\rho g\beta[T-T_0] \quad (3)$$

$$\frac{\partial(\rho uT)}{\partial x}+\frac{\partial(\rho vT)}{\partial y}=\Gamma\left[\frac{\partial^2 T}{\partial x^2}+\frac{\partial^2 T}{\partial y^2}\right],\ \Gamma=\frac{k}{c} \quad (4)$$

The associated boundary conditions for the above equations are [5]:

- At x = 0, $\frac{\partial T}{\partial x}=0$; $\frac{\partial v}{\partial x}=0$ ,At x = $D_h/2$ u = v = 0 (5)
- At y = 0 u = 0 , $v=\bar{v}$ , $T=T_0$ (6)
- At $0 \le y \le L_h$ ( Heated section ) $q''=k\frac{\partial T}{\partial x}$ (7)
- At $L_h \le y \le L_i$ (Insulated section ) $-k\frac{\partial T}{\partial x}=0$ (8)
- At $y = y_L$ $\frac{\partial u}{\partial y}=\frac{\partial v}{\partial y}=\frac{\partial T}{\partial y}=0$ (9)

Equation (6) prescribe a uniform velocity and a uniform temperature at the channel entrance, and equation (9) assumes the stream wise energy diffusion flux to be negligible and fully developed velocity profiles at the outlet.

**Friction Factor and Nusselt Number**

The definitions of two physical parameters of practical importance are introduced here. The first is the friction factor $f$ , which is given by the following expression [3].

$$f=-\frac{2}{\mathrm{Re}_L}\left(\frac{\partial v}{\partial x}\right)_{x=D_h/2} \quad (10)$$

where $\mathrm{Re}_L$ is the local Reynolds number defined as, $\mathrm{Re}_L=\frac{\rho\bar{v}D_h}{\mu}$ (11)

The second parameter of interest is the local Nusselt number, defined as [3]:

$$Nu_L=\frac{q''D_h}{k(T_w-T_b)} \quad (12)$$

Were the bulk temperature is defined as [4]:

$$T_b=\frac{\int_0^{D_h/2}\rho C_p vT dx}{\int_0^{D_h/2}\rho C_p v dx} \quad (13)$$

The above equations are put in dimensionless form by defining the following variables:

$$X=\frac{x}{D_h}\ ;\ Y=\frac{y}{D_h}\ ;\ U=\frac{u}{\bar{v}}\ ;\ V=\frac{v}{\bar{v}} \quad (14)$$

$$\theta = \frac{T\text{-}T_0}{q'' \frac{D_h}{k}} \quad ; \quad P = \frac{p + p_0}{\rho_0 \bar{v}^2} \quad ; \tag{15}$$

Using the above defined variables, the governing equations can be casted in dimensionless form as:

$$\frac{\partial(U)}{\partial X} + \frac{\partial(V)}{\partial Y} = 0 \tag{16}$$

$$\frac{\partial(UU)}{\partial X} + \frac{\partial(UV)}{\partial Y} = -\frac{\partial P}{\partial X} + \frac{1}{\mathrm{Re}}\left[\frac{\partial^2 U}{\partial X^2} + \frac{\partial^2 U}{\partial Y^2}\right] \tag{17}$$

$$\frac{\partial(UV)}{\partial X} + \frac{\partial(VV)}{\partial Y} = -\frac{\partial P}{\partial Y} + \frac{1}{\mathrm{Re}}\left[\frac{\partial^2 V}{\partial X^2} + \frac{\partial^2 V}{\partial Y^2}\right] + \frac{Gr}{\mathrm{Re}^2}\theta \tag{18}$$

$$\frac{\partial(U\theta)}{\partial X} + \frac{\partial(V\theta)}{\partial Y} = \frac{1}{\mathrm{Pr}\,\mathrm{Re}}\left[\frac{\partial^2 \theta}{\partial X^2} + \frac{\partial^2 \theta}{\partial Y^2}\right] \tag{19}$$

The dimensionless form of the boundary conditions can be written as:

- At , X = 0 $\frac{\partial \theta}{\partial X} = 0$; and At X =1 U = V = 0 (20)
- At Y = 0 , $V = 1$ ; $\theta$ = 0 (21)
- $0 \le Y \le L_h/D_h$ (Heated section ) $\frac{\partial \theta}{\partial X} = 1$ (22)
- $L_h/D_h \le Y \le L_i/D_h$ ( Insulated section ) $\frac{\partial \theta}{\partial X} = 0$ (23)
- $Y = Y_L/D_h$ $\frac{\partial U}{\partial Y} = \frac{\partial V}{\partial Y} = \frac{\partial \theta}{\partial Y} = 0$ (24)

Friction factor and Nusslet number, equations (10; 12) can be written as:

$$f = -\frac{2}{\mathrm{Re}_L}\left(\frac{\partial V}{\partial X}\right)_{X=1} \quad ; \quad Nu_L = \frac{1}{(\theta_w - \theta_b)} \tag{25}$$

## NUMERICAL SOLUTION

The solution of the conservation equations of mass, momentum and energy is obtained by expressing the dimensionless form of these equations and the associated boundary conditions in a discrete form using finite volume method [1] and the simple procedure is adopted for the linkage of velocities and pressure through the continuity equation. In this method, the computational domain is divided into a number of non-overlapping control volumes, where pressure and temperature are stored at the center of each cell, while the velocity components, u and v are stored at the control volume faces (staggered grid) to avoid checkerboard pressure field [19]. The governing equations were discretized to produces a set of linear algebraic equations which are solved simultaneously with the tridiagonal matrix algorithm (TDMA). The line by line method has been used where the domain is covered by a number of sweeps in the x- and y directions. A uniform mesh is employed in both the axial and transverse directions and sufficient grid distribution was used to ensure that results are independence of mesh size. Figure (2) shows the results of the friction factor for different mesh size and 50 by 500

grid distribution was found optimum for acceptable results. The mass source residual, R, which is defined as the sum of the absolute values of the net mass fluxes into and out of every control volume is used as convergence criterion. The code stops if the mass source residual falls below $10^{-6}$. The converged solution for forced convection was checked against the exact solution of the velocity profile at the channel out let (parabolic) a good agreement was noticed.

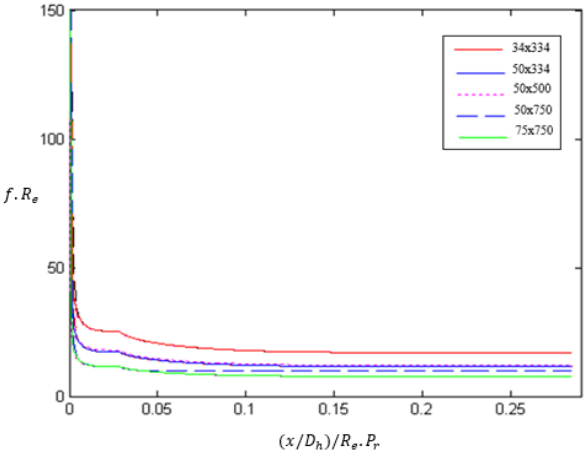


**Figure 2: Friction factor values for different grid sizes.**

## RESULTS AND DISCUSSIONS

As mentioned previously, the objective of this work is to determine the combined effects of mixed convection on hydrodynamic and thermal fields for partially heated vertical channels. This objective was achieved by computing velocity and temperature profiles, friction factor and Nusselt number. Isotherms and streamlines were plotted for different values of Grashof number. It is worth mentioning here that the results of the present study were for the range of $10^5 \leq |Gr| \leq 10^7$; Re = 500, Pr = 0.7 and $L_h/D_h = 10$. Note that in order to acheve parabolic profiles for velocity and temperature, the length of the insulated section was set as $L_{in}/D_h = 90$. For given Gr.

### Grid-independence

For the purpose of grid independence test, the values of Re and G*r* for mixed convection were chosen as 500 and $10^5$ respectively. Grid independence is established by monitoring the friction factor values for different grid sizes. In choosing the optimum mesh for the converged results, the number of control volumes for successive grids were increased roughly by a factor of 1.5 in each direction. The results of the grid variation study are presented in Figure (2), based on these results, a mesh of 50 control volume in the x- direction by 500 control volume in the y- direction was adopted for the rest of all simulations

It is evident from Figure (3a), Figure (3b), and Figure (3c) that the velocity, v, is zero at the wall due to no-slip condition. In addition, these figures display the axial velocity profile in the heated part of the channel for aiding buoyancy flow, and show the axial velocity distribution at two axial positions for different values of Grashof number that represent the ratio of the bouncy forces to the viscous forces.

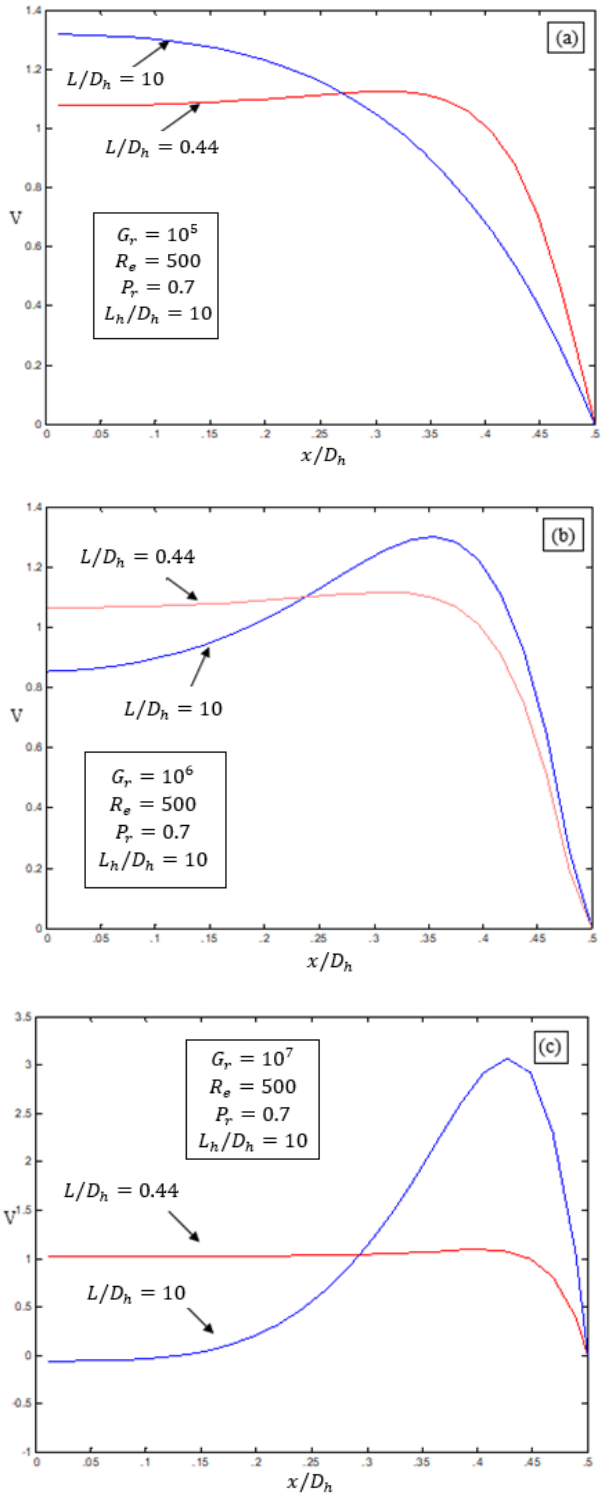


**Figure 3: Axial velocity profiles for (a) $Gr = 10^5$, (b) $Gr = 10^6$ and (c) $Gr = 10^7$.**

For $Gr = 10^5, 10^6$ and $10^7$ the velocity distribution behaves differently, at low value of G*r* the flow is dominated by forced convection and the shape of the velocity curve far enough from the entrance is approximately equivalent to the fully developed channel flow; this is shown in Figure (3a). However, at moderate values of Grashof number where the combined effect of natural and forced convection contributes equally to the flow, the

velocity distribution at the same axial location deviates from the fully developed case. This is shown in Figure (3b), as can be seen, the velocity drops at the center of the channel, attain it is maximum value at some location near the wall and sharply drops to zero exactly at the wall of the channel. It is very interesting to observe that the Boussinesq approximation (constant properties) underestimates systematically the fluid axial velocity. This effect is negligible in the vicinity of the inlet section, where the fluid temperature is relativity low. The underestimation of the velocity values increases considerably with the increase of $Gr$ , as shown in Figure (3c) for $Gr = 10^7$ and $L/D_h = 10.0$ .At this axial location the dimensionless axial velocity on the channel centerline is dropped to about -0.055 and increases to its maximum value of 3.0. Thus one may expect that, this value of critical $Gr$ corresponding to the onset of the reverse flow.

Figure (4c) with $Gr = 10^7$ shows that the hydrodynamic field is different from that corresponding to pure forced convection. As the fluid moves downstream, the distortion of the velocity profile becomes larger. As expected, the acceleration of the fluid particles near the wall is compensated by deceleration at the axis of the channel. Seeing that $Gr/\mathrm{Re}^2$ is bigger than unity in this case (i.e. the inertia forces less important than the buoyancy forces), the deceleration causes a reversal flow characterized by a negative axial velocity in the central part of the channel.

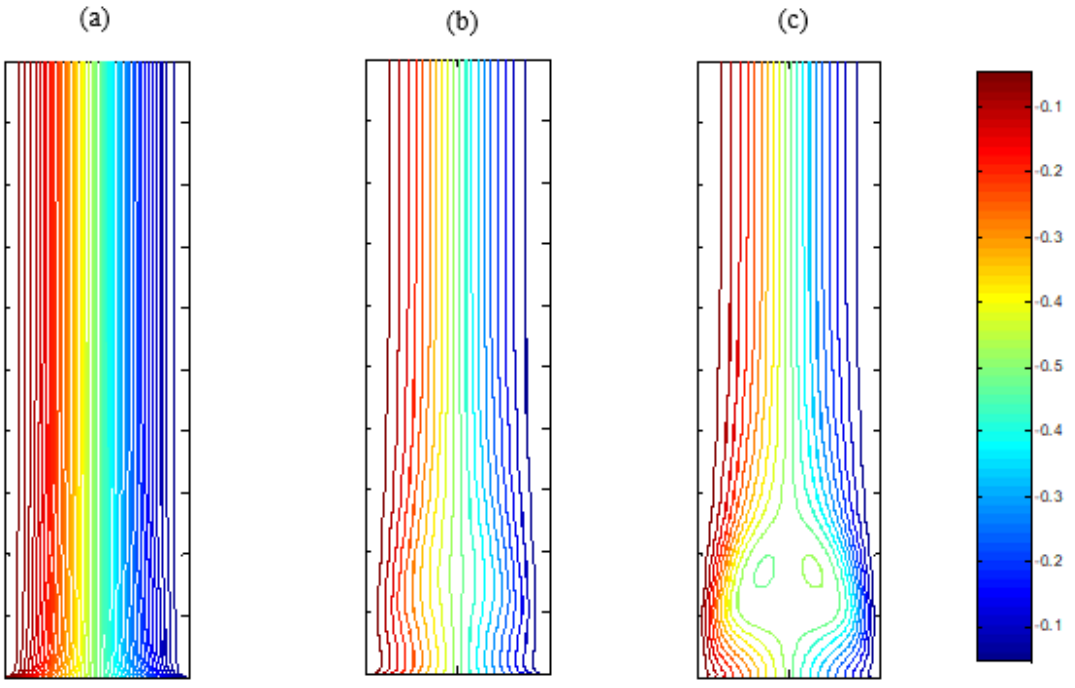


**Figure 4: Streamlines for aiding buoyancy at (a) $Gr = 10^5$,(b) $Gr = 10^6$ and (c) $Gr = 10^7$.**

The location, the size and the shape of the recirculation zones at various $Gr$ numbers are clearly shown in the streamlines plot, Figure (4a), Figure (4b), and Figure (4c). The stationary recirculation cells expand in both the x and y directions and move toward the entrance with increasing $Gr/\mathrm{Re}^2$ ratio. It is interesting to mention that the flow reversal originating in the heated section terminates at some downstream location in

the insulated zone. It should be noted that, the reverse flow does not exist for low value of G*r* as shown in Figure (4a) where forced convection dominates the flow, but the recirculation zone starts to develop as the value of G*r* increased to a certain value where both natural and forced convection effects have considerable effect. This is shown in Figure (4b) where the reverse flow just starts to originate at the channel entrance.

Figure (5) shows the axial evolution of the product $f.\mathrm{Re}$ for the cases considered earlier. Since the friction factor is directly related to the velocity gradient on the channel wall, equation (10). In the aiding case (see Figure 5) a maximum value of this product occurs at the point where the flow reversal starts. The location of the maximum friction factor in Figure (5) move upstream when the heat flux, or equivalently *Gr* number, increases. It is interesting to note that the wall shear stress increases with increasing $Gr/\mathrm{Re}^2$ in the aiding case.

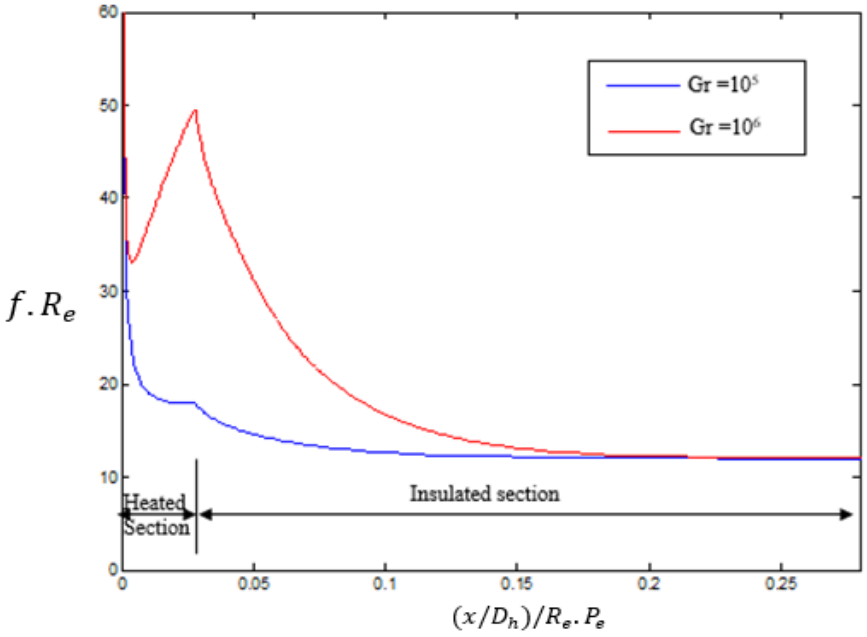


**Figure 5: Local friction factors for aiding buoyancy.**

Figure (6a), Figure (6b), and Figure (6c) display the temperature profiles at various axial locations for aiding bouncy flow. These figures show that the fluid upstream from the recirculation cell is warmer at the vicinity of the wall than anywhere else. Its temperature decreases monotonically from the wall to the axis where it takes its minimum value. However the fluid temperature presents a minimum at $x = 0.25D_h$ for axial position corresponding to the location of the recirculation cell; Figure (6c).

In summary, the effect of the convection mode on the temperature profile is clearly demonstrated by the above mentioned figures, where the temperature at the vicinity of the wall is compared for each case. Figure (6a) shows higher temperature at the channel wall (forced convection) than the value shown in Figure (6c) where natural convection dominates.

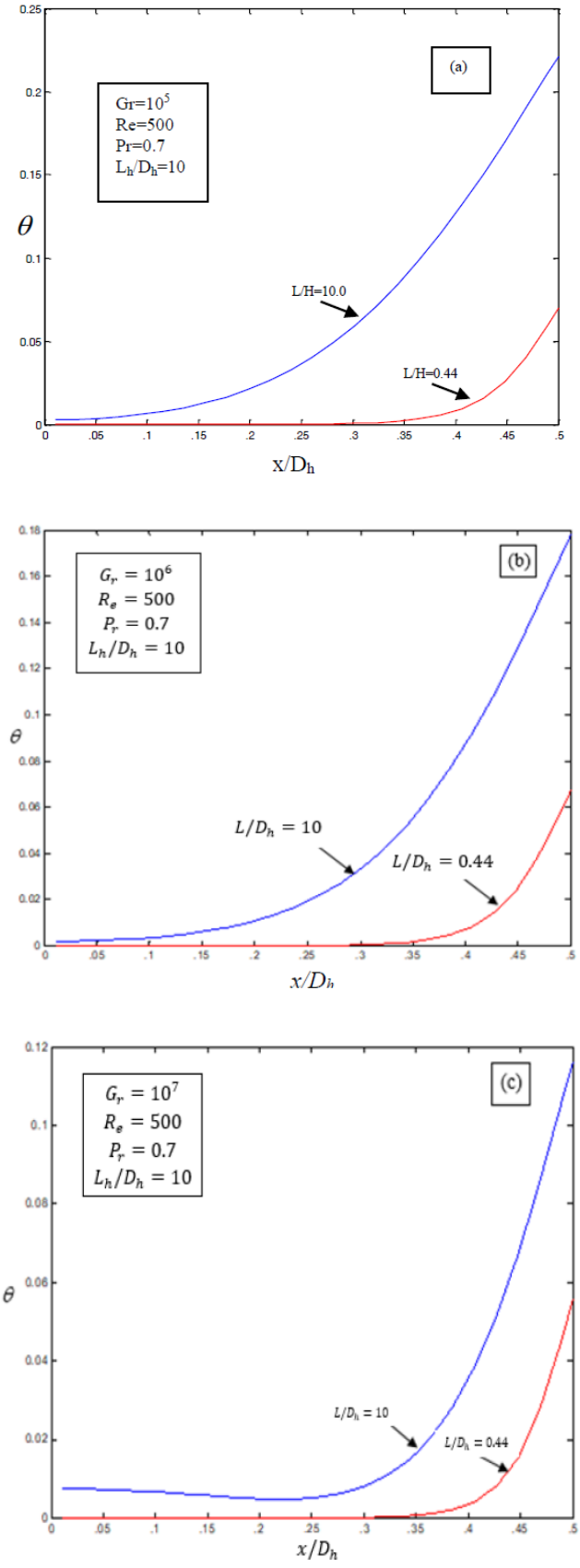


**Figure 6: Temperature profiles for (a) $Gr = 10^5$, (b) $Gr = 10^6$ and (c) $Gr = 10^7$**

Figure (7a), Figure (7b), and Figure (7c) shows the isotherms in the channel at different values of Grashof numbers, G*r*. As can be seen, the contours are more flattened for G*r* = $10^7$, this attributed to the fact that, the combined effects of free and forced convection must be considered when the ratio Gr/$Re^2$ is approximately equal to unity. This ratio is much higher than unity in Figure (7c), where forced convection has little effects in the flow field for higher G*r*.

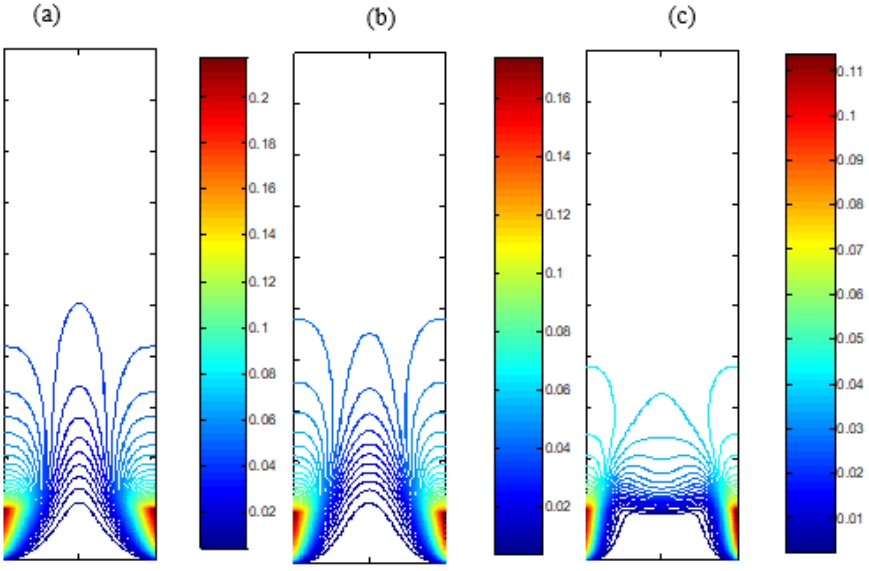


**Figure 7: Isotherms for (a)** $Gr = 10^5$**, (b)** $Gr = 10^6$ **and (c)** $Gr = 10^7$ **.**

The axial evolution of the local Nusselt number is displayed in Figure (8) for various G*r* numbers. For aiding buoyancy, Figure (8) shows that, the Nusslet number decreases and reaches asymptotic values as soon as the flow becomes fully developed.

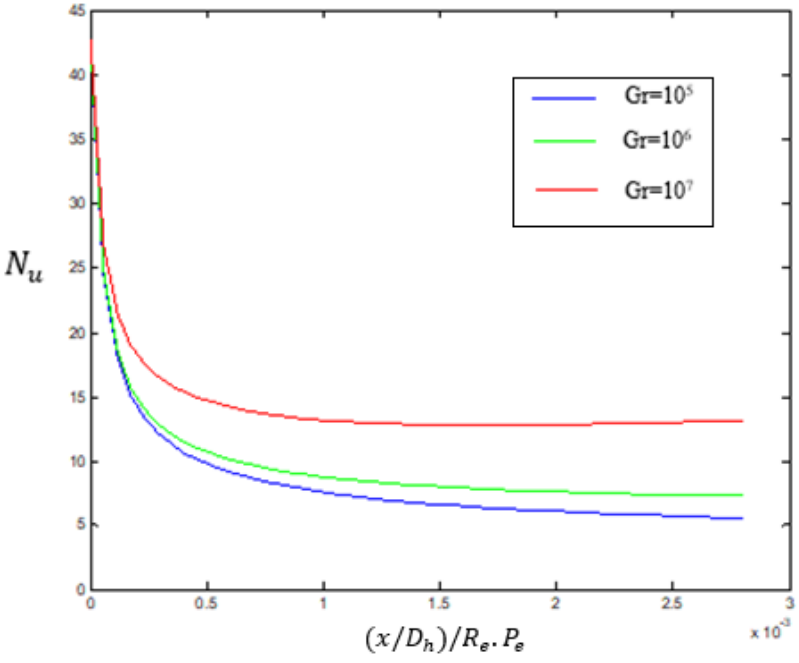


**Figure 8: The axial evolution of the local Nusselt number for various Gr numbers.**

The asymptotic value increases with increasing $Gr/\mathrm{Re}^2$ ratio. On the other hand, for opposing buoyancy reversal that before reaching its asymptotic value, the Nusslet number reaches a minimum value which occurs at the separation point of the boundary layer. At this point the velocity is very small and heat transfer takes place essentially by conduction. The position of the minimum seems to vary with $Gr/\mathrm{Re}^2$ . Then the Nusselt number increases reach its asymptotic value which does not appear on the figure because the recirculation zone terminates in the insulated zone where Nusselt drops to zero.

## CONCLUSIONS

The aim of this study is to investigate numerically laminar mixed convection in partially heated vertical channel. The case of assisting flow is considered and part of the channel is subjected to uniform heat flux. The effect of the length of the heated section on the flow pattern and heat transfer performance is examined for a range of Grashof numbers. The influence of axial diffusion was taken into account in the momentum and energy equations and particular attention is given to the ratio $Gr/\mathrm{Re}^2$ and it's relevant to flow reversal in the entrance region of the channel. The effect of aiding bouncy forces on the hydrodynamic and thermal fields has been demonstrated for air with Re = 500, $10^5 \le Gr \le 10^7$ and Pr = 0.7. Flow reversal was observed near the axis in the case of upward heated flow (aiding buoyancy). The numerical results presented, revealed some interesting features which may be summarized as:

1. The effects of the heated part of the channel on the hydrodynamic and thermal fields are demonstrated for $\left| Gr \right| \ge 10^5$ for aiding flow.
2. Nusselt number approaches the asymptotic value at the vicinity of the channel wall for $Gr \le 10^5$. For $Gr \ge 10^6$ the Boussinesq approximation over predicts the overall heat transfer rate.
3. For $Gr$ up to $4*10^5$ The Boussinesq approximation still predicts reasonably the heat transfer rate.
4. In general, the heated section modifies the flow field and hence the wall convective heat transfer.

## REFERENCES


[1] Aung, W., Moghadam, H.E., "Simultaneous Hydrodynamic and thermal developing in mixed convection in a vertical annulus with fluid property variations", Trans ASME, J. Heat transfer Vol 113, 1989, 926-930.

[2] Gebhart, B., Jaluria, Y., Mahajan, R. et Sammakia B., "Buoyancy-induced flows and transport" New York, Hemisphere Publishing, 1988.

[3] Incropera, Frank, P., DeWitt, David, P., "Fundamentals of Heat and Mass Transfer", 6th ed, John Wiley 2007.

[4] Bejan, A., "Convection heat transfer", 3th ed. John Wiley & Sons Inc, 2004.

[5] Desrayaud, G., Lauriat, G. "Flow reversal of laminar mixed convection in the entry region of symmetrically heated, vertical plate channels", International Journal of Thermal Sciences, 48(11), 2009, 2036–2045.

[6] Laaroussi, N., Lauriat, G., Desrayaud, G. "Effects of variable density for film evaporation on laminar mixed convection in a vertical channel", International Journal of Heat and mass Transfer, 52(1), 2009, 151–164.

[7] Patankar, S. V.,"Numerical Heat Transfer and Fluid Flow", McGraw-Hill, 1980.

[8] Elenbaas, W., "Heat dissipation of parallel plates by free convection", Physica 9 1942, 1–28.

[9] Dehghan, A. A., Behnia, M., "Combined natural convection–conduction and radiation heat transfer in a discretely heated open cavity", ASME J. Heat Transfer Vol 118, 1996, 56–64.

[10] Chen, T., Armaly, B., Aung, W., "Natural Convection: Fundamentals and Applications", 1985, 669–725.

[11] Anand, N.K., Kim, S.H., Aung, W., "Effect of wall conduction on free convection between asymmetrically heated vertical plates: uniform wall temperature", Int. J. Heat Mass Transfer Vol 33 ,1990, 1025–1028.

[12] Kim, S.Y., Sung, H.J., Hyun, J.M., "Mixed convection from multiple layered boards with cross-stream wise periodic boundary conditions", Int. J. Heat Mass Transfer 35 (11), 1992, 2941–2952.

[13] Rao, G. M., Narasimham, G.S., "Laminar conjugate mixed convection in a vertical channel with heat generating components". International Journal of Heat and Mass Transfer Vol 50, 2007, 3561–3574.

[14] Aung, W., Moghadam, H. E., "Simultaneous Hydrodynamic and thermal developing in mixed convection in a vertical annulus with fluid property variations", Trans ASME, J. Heat transfer Vol 113, 1989, 926-930.

[15] Braaten, M. E., Patankar, S. V., "Analysis of laminar mixed convection in shrouded arrays of heated blocks, International Journal of Heat and Mass Transfer", 28 (9), 1985, 1699–1709.

[16] Tu¨rkolu, H., Yu¨N., cel, "Mixed convection in vertical channels with a discrete heat source", Heat and Mass Transfer Vol 30, 1995, 159–166.

[17] Wang, Y., Vafai, K., "Heat transfer and pressure loss characterization in a channel with discrete flush-mounted and protruding heat sources", Experimental Heat Transfer Vol 12, 1999, 1–16.

[18] Nesreddine, H., Galanis, N., "Recirculating flow in aiding/ opposing mixed convection in vertical pipes", Numerical Heat Transfer, Part A, 1997, 575-585.

[19] Hornbeck, R. W., "An All- Numerical method for heat transfer in the inlet of a tube", ASME, 1965, Paper 65- WA/HT-36.

**NOMENCLATURE**

$A$ flow cross section area ($m^2$)

$C$ specific heat (kJ/kg K)

$f$ friction factor

G$r$ Grashof number based on heat flux

$D_h$ hydraulic diameter of the channel (m)

$h$ heat transfer coefficient

$L_h$ length of the heated section (m)
$L_i$ length of the insulated section (m)
Nu local Nusselt number
P pressure (kPa)
P dimensionless pressure
$P_e$ Peclet number,$R_e P_r$
$P_r$ Prandtl number
$\overline{\overline{q}}$ heat flux at the wall (W/m$^2$)
Re Reynolds number
T temperature
$T_w$ wall temperature
$T_b$ bulk temperature
$u$ velocity components in x-direction (m/s)
$v$ velocity components in y-direction (m/s)
$u$ dimensionless Velocity in x-direction (m/s)
$V$ dimensionless Velocity in y-direction
$\overline{v}$ mean velocity (m/s)
$x, y$ Cartesian coordinates

**Greek symbols**

$\beta$ thermal expansion coefficient (K$^{-1}$)
$k$ thermal conductivity (W/$m.k$)
$\theta$ dimension less temperature
$\mu$ dynamic viscosity ($Pa.\sec$)
$v$ kinematic viscosity (m$^2$/sec)
$\rho$ density (kg/m$^3$)
$\alpha$ thermal diffusivity (m$^2$/sec)

**Subscript**

0 evaluated at the inlet temperature